Supporting Information

Visual Detection of Fluoride anions Using Mixed Lanthanide Metal-Organic Frameworks with a Smartphone

Xiaoliang Zeng†, Jing Hu†, Meng Zhang‡, Fenglei Wang‡, Li Wu*†, Xiandeng Hou*†‡

† Analytical & Testing Center, Sichuan University, Chengdu, Sichuan 610064, China

‡ College of Chemistry and Key Laboratory of Green Chemistry and Technology of MOE, Sichuan University, Chengdu, Sichuan 610064, China

*E-mail: wuli@scu.edu.cn， houxd@scu.edu.cn

Table of Contents

1. Characterization of prepared MOFs

1.1. Crystal structures of Ln-MOFs

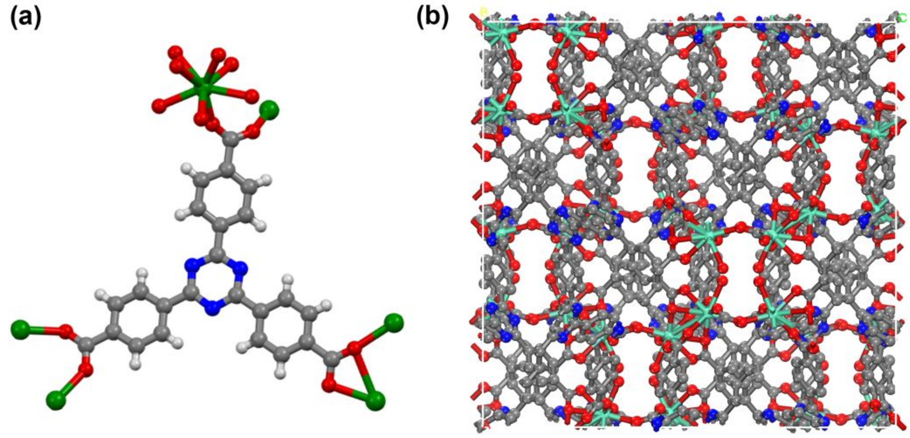

Figure S1[1]**.** (a) Coordination mode of $TATB^{3-}$ ligands and Tb^{3+} (Tb green, C gray, O red, N blue; H light grey). Each Tb^{3+} ion coordinates to one water oxygen atom and seven carboxylic oxygen atoms from six $TATB^{3-}$ forming a distorted bicapped triprismatic coordination geometry. (b) Crystal structure of Tb(TATB) viewed along the *bc* plane (Tb green, C gray, O red, N blue; all H atoms are omitted for clarity).

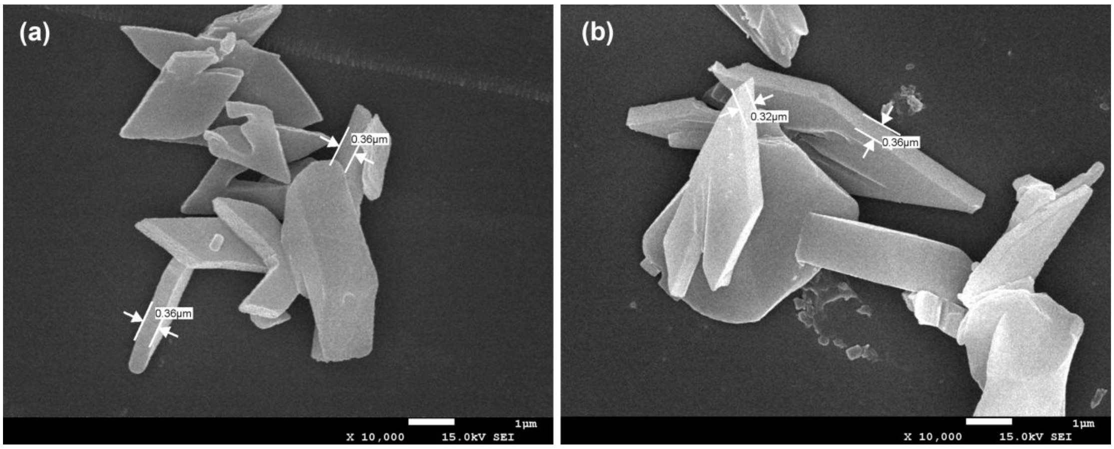

Figure S2. SEM images of synthesized Ln-MOFs a) Ln-MOFs **1** and b) Ln-MOFs **4**.

1.2. Mixed Ln-MOF digestion procedures and Tb^{3+}/Eu^{3+} ratio determination

The molar ratios of Tb^{3+}/Eu^{3+} contained in mixed Ln-MOFs were determined by inductively coupled plasma-optical emission spectrometry (ICP-OES) with an ARCOS FHS12 (SPECTRO Analytical Instruments Inc., Germany). Sample digestion and acid evaporation were performed before the analysis by ICP-OES. Typically, each kind of MOF sample (2 mg) was dissolved in a 5 mL mixture of concentrated HNO_3 and HCl (v/v=3:1) and heated at 200 ^{o}C for 1 h. After that, the solution was evaporated at 150 ^{o}C for 10 min and the residue was diluted to 10 mL with 2% HCl solution (v/v).

Table S1. Tb^{3+}/Eu^{3+} ratios determined by ICP-OES

MOF	Tb^{3+} (ppm)	Eu^{3+} (ppm)	Tb^{3+}/Eu^{3+} ratio
Ln-MOFs **4**	13.353	0.412	97:3
Ln-MOFs **5**	12.687	0.620	95:5
Ln-MOFs **6**	12.374	1.374	90:10

1.3. Luminescent decay curves and lifetime measurements

Luminescent decay curves were obtained with an Fluorolog-3 spectrofuorometer (Horiba Jobin Yvon) equipped with a spectra LED (280 nm, S-280, Horiba Scientific) as the excitation source. The data were fitted with the second order exponential decay. The efficiency of energy transfer (η_T) from Tb^{3+} to Eu^{3+} can be calculated based on the following equation: $\eta_T = 1 - (\tau/\tau_0)$, where τ and τ_0 is the luminescent lifetime of Tb^{3+} in Ln-MOFs **4** and Ln-MOFs **1**, respectively.[2]

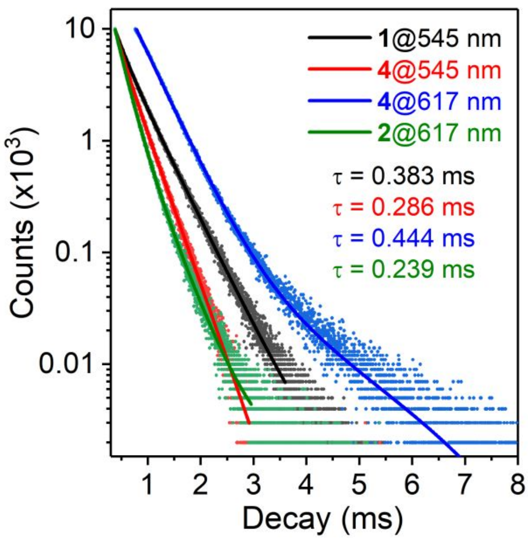

Figure S3. Luminescent decay curves of synthesized Ln-MOFs. Black line: Ln-MOFs **1**, red line and blue line: Ln-MOFs **4**; green line: Ln-MOFs **2**.

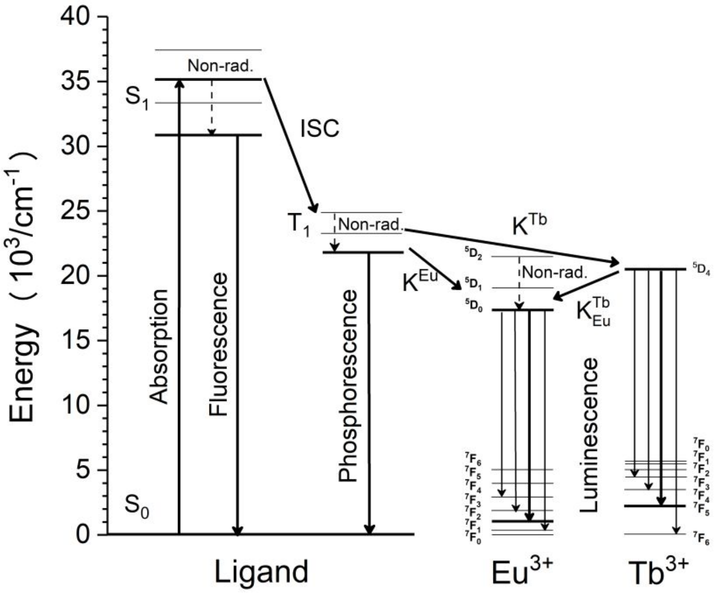

Figure S4. The schematic representation of energy transfer pathways in Tb/Eu(TATB). Abbreviations: S_0 = singlet ground state; T_1 = triplet excited state; k = nonradiative transition probability.

2. Ratiometric detection of fluoride ions

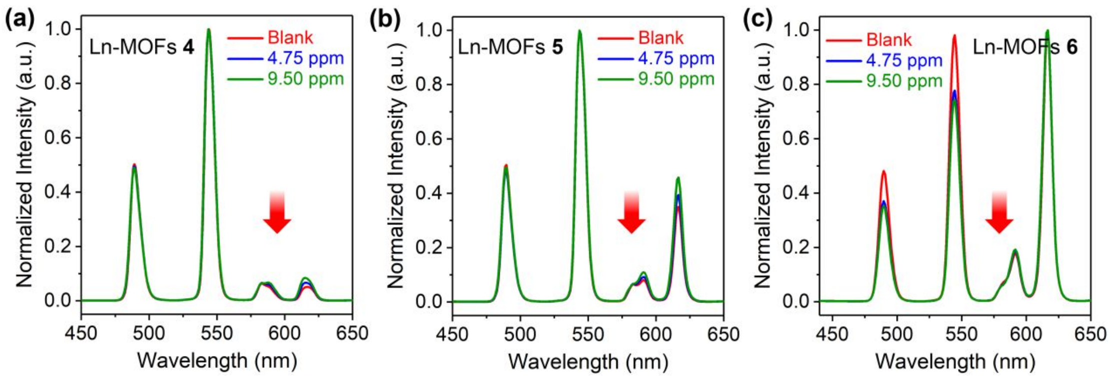

Figure S5. The emission spectra of synthesized mixed Ln-MOFs treated with different concentrations of fluoride ions under the excitation at 320 nm. (a) Ln-MOFs **4**; (b) Ln-MOFs **5**; (c) Ln-MOFs **6**.

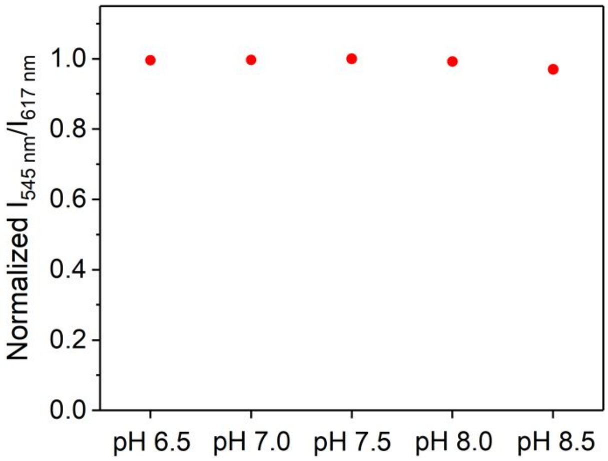

Figure S6. The emission intensity ratio ($I_{545\ nm}/I_{617\ nm}$) of Ln-MOFs **4** in solutions with different pH values.

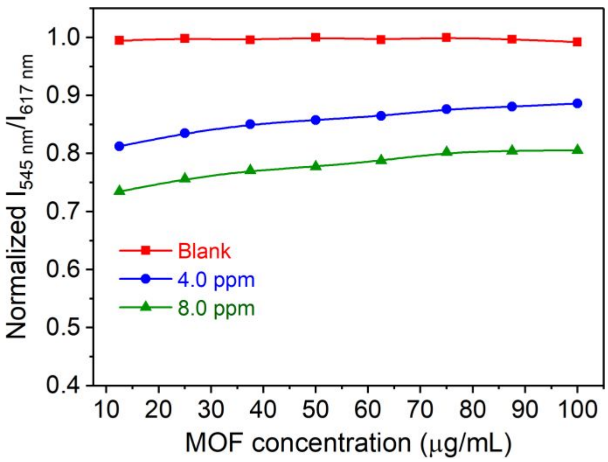

Figure S7. The normalized emission intensity ratio ($I_{545\ nm}/I_{617\ nm}$) of Ln-MOFs **4** with different concentrations of MOFs.

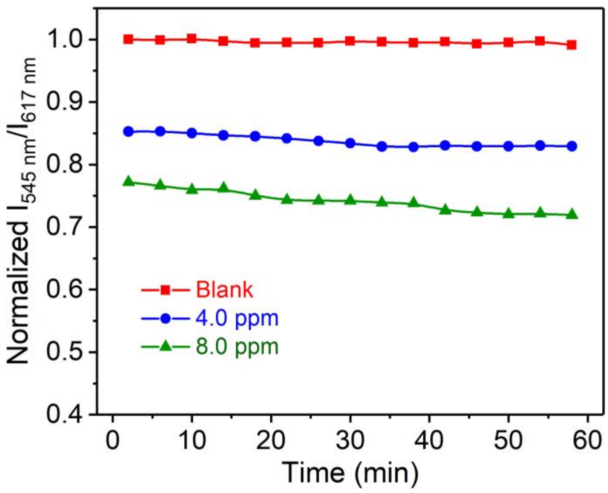

Figure S8. The normalized emission intensity ratio ($I_{545\ nm}/I_{617\ nm}$) of Ln-MOFs **4** with different incubation time.

3. Sensing mechanism of the ratiometric sensor

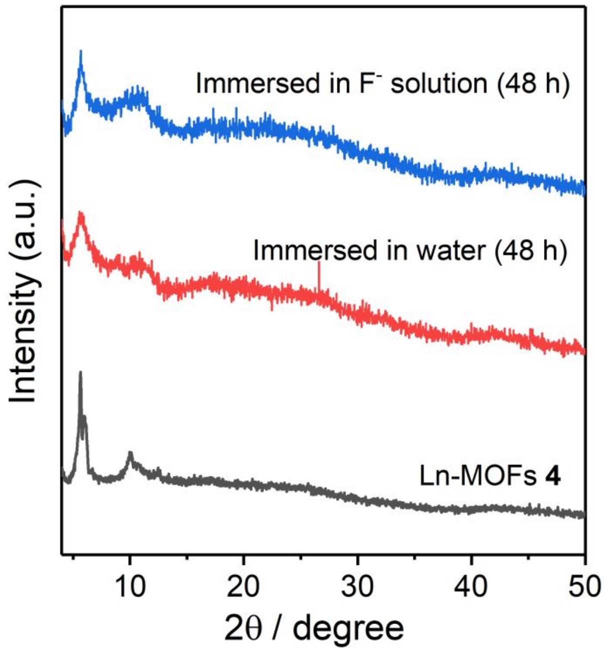

Figure S9. PXRD patterns of Ln-MOFs **4** and Ln-MOFs **4** treated with water and fluoride solution (10 ppm), respectively.

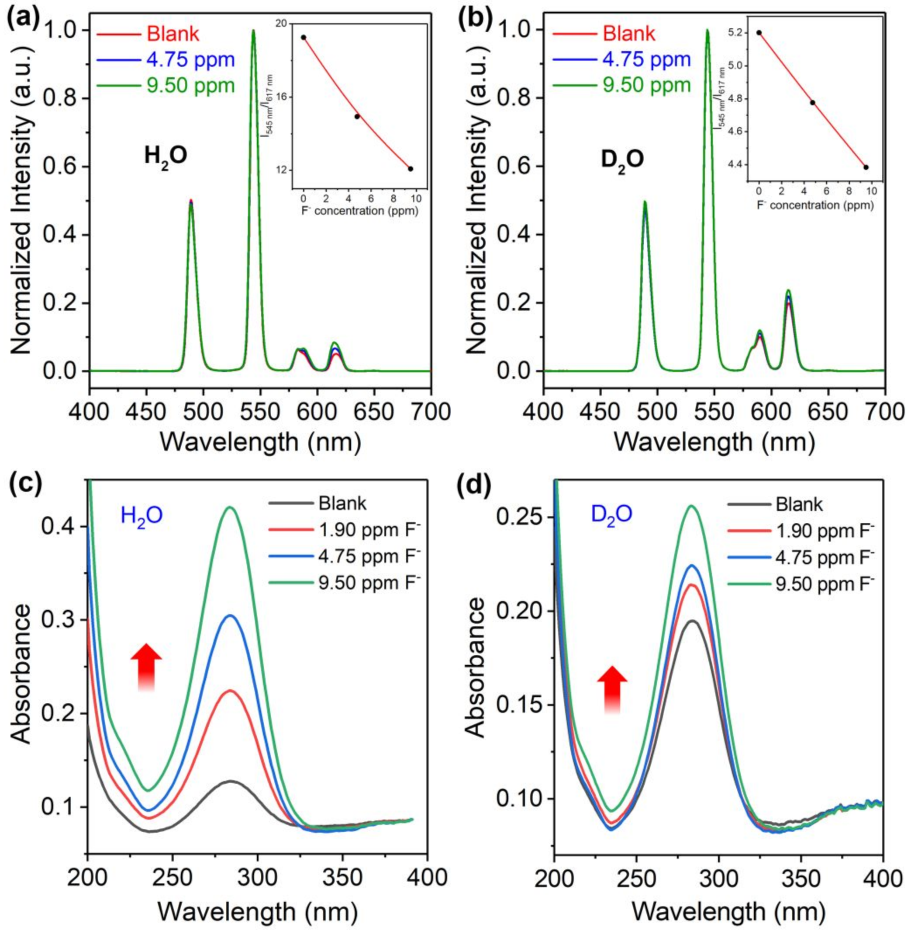

Figure S10. Luminescence emission spectra of Ln-MOFs **4** after addition of fluoride ions in the medium of water (a) and heavy water (b), respectively. The inset figures are corresponding changes in $I_{545\ nm}/I_{617\ nm}$ versus the concentration of F^-. UV-Vis absorption spectra of Ln-MOFs **4** after addition of fluoride ions in the medium of water (c) and heavy water (d), respectively.

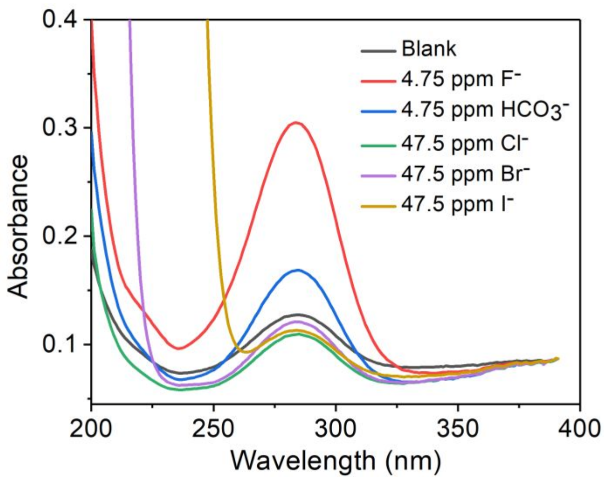

Figure S11. UV-Vis absorption spectra of Ln-MOFs **4** after addition of various anions.

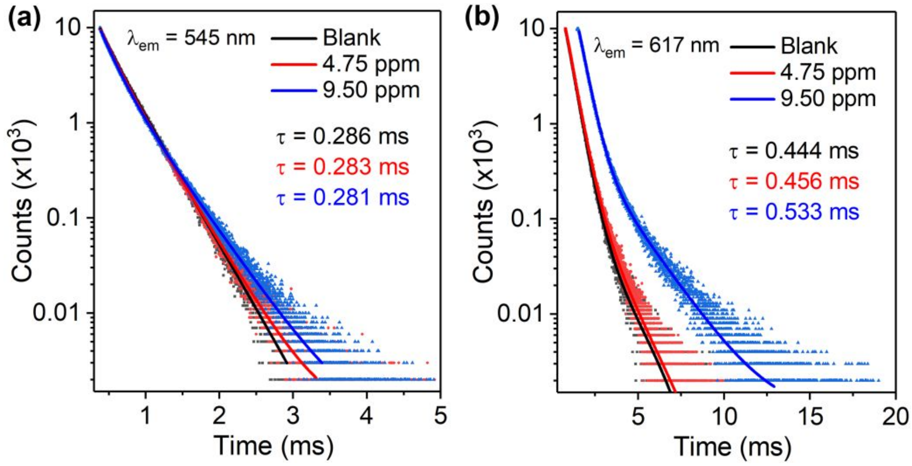

Figure S12. Luminescent decay curves of Ln-MOFs **4** after addition of different concentrations of fluoride ions. (a) Monitored at 545 nm; (b) Monitored at 617 nm. The data were fitted with the second order exponential decay.

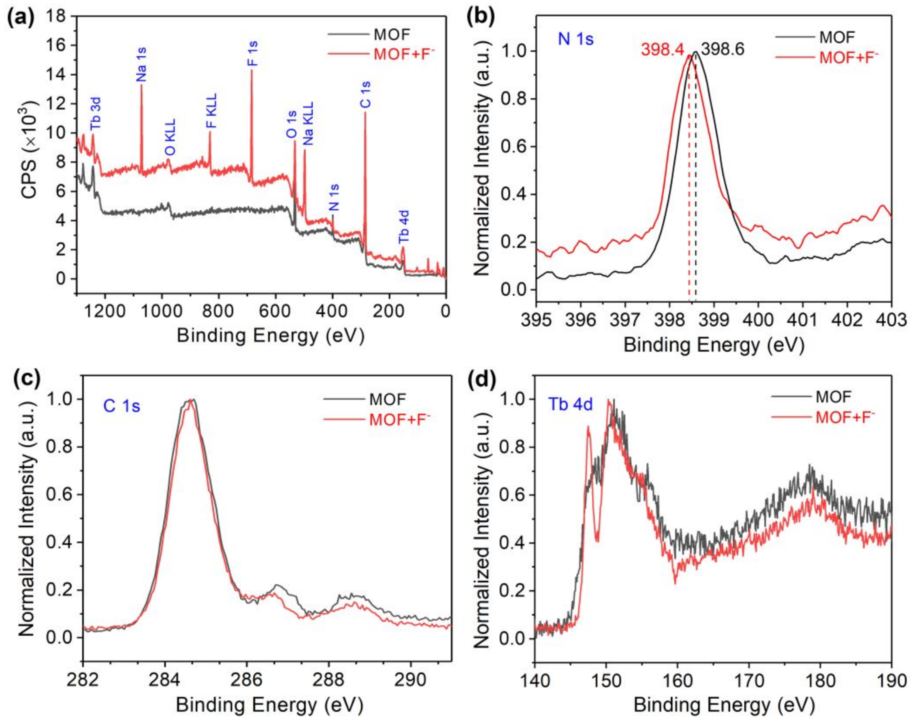

Figure S13. XPS spectra of Ln-MOFs **4** before and after being treated with F^-, respectively. (a) Full spectra; (b) N 1s spectra; (c) C 1s spectra; (d) Tb 4d spectra.

4. Visual detection of fluoride and sample analysis

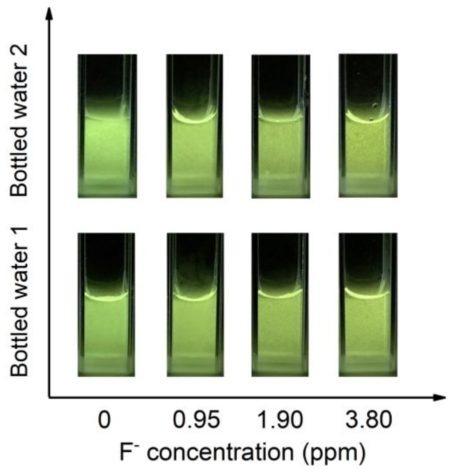

Figure S14. Visual detections of F^- in bottled water samples. The photos were taken with a smartphone under a 310 nm LED lamp.

Table S2. Fluoride content in bottled water samples (n=3)

Sample	Added (ppm)	This method				By ion chromatography (ppm)
		Found with fluorometer (ppm)	Recovery	Found with smartphone (ppm)	Recovery	
Sample-1	--	0.11 ± 0.10	--	n.d.	--	<0.10
	0.95	0.94 ± 0.11	87.4%	1.07 ± 0.16	113%	0.94
	1.90	1.63 ± 0.13	80.1%	1.97 ± 0.32	104%	1.86
	3.80	--	--	3.59 ± 0.16	94.5%	3.64
Sample-2	--	n.d.	--	n.d.	--	<0.10
	0.95	0.85 ± 0.04	89.5%	1.12 ± 0.14	118%	0.93
	1.90	1.62 ± 0.13	85.3%	2.22 ± 0.32	113%	1.88
	3.80	--	--	3.47 ± 0.38	91.3%	3.72

Table S3. Comparison of Ln-MOFs **4** with existing MOF-based F^- sensors.

System	Sensitivity	Selectivity	Ratiometric detection	Visual detection by RGB value	Reference
Fluorescein @MOF	15 ppb	Good	No	No	[3]
MOF-76	1900 ppb	Moderate	No	No	[4]
Boric acid MOF	67 ppb	Good	Yes	No	[5]
SION-105	9.1 ppb	Good	No	No	[6]
Ln-MOFs **4**	96 ppb	Good	Yes	Yes	This work

5. References

1. Zhang, H.; Li, N.; Tian, C.; Liu, T.; Du, F.; Lin, P.; Li, Z.; Du, S., Unusual High Thermal Stability within A Series of Novel Lanthanide TATB Frameworks: Synthesis, Structure, and Properties (TATB = 4,4′,4″-s-Triazine-2,4,6-triyl-tribenzoate). *Cryst. Growth Des.* **2012,** *12*, 670-678.

2. Zhou, J.; Li, H.; Zhang, H.; Li, H.; Shi, W.; Cheng, P., A Bimetallic Lanthanide Metal–Organic Material as a Self-Calibrating Color-Gradient Luminescent Sensor. *Adv. Mater.* **2015,** *27*, 7072-7077.

3. Hinterholzinger, F. M.; Rühle, B.; Wuttke, S.; Karaghiosoff, K.; Bein, T., Highly Sensitive and Selective Fluoride Detection in Water through Fluorophore Release from A Metal-Organic Framework. *Sci. Rep.* **2013,** *3*, 2562.

4. Chen, B.; Wang, L.; Zapata, F.; Qian, G.; Lobkovsky, E. B., A Luminescent Microporous Metal–Organic Framework for the Recognition and Sensing of Anions. *J. Am. Chem. Soc.* **2008,** *130*, 6718-6719.

5. Yang, Z.-R.; Wang, M.-M.; Wang, X.-S.; Yin, X.-B., Boric-Acid-Functional Lanthanide Metal–Organic Frameworks for Selective Ratiometric Fluorescence Detection of Fluoride Ions. *Anal. Chem.* **2017,** *89*, 1930-1936.

6. Ebrahim, F. M.; Nguyen, T. N.; Shyshkanov, S.; Gładysiak, A.; Favre, P.; Zacharia, A.; Itskos, G.; Dyson, P. J.; Stylianou, K. C., Selective, Fast-Response, and Regenerable Metal–Organic Framework for Sampling Excess Fluoride Levels in Drinking Water. *J. Am. Chem. Soc.* **2019,** *141*, 3052-3058.